Detection of Surge and Stall in Compression Systems: An Example Study

Yew-Wen Liang and Der-Cherng Liaw

***Abstract*—Issues concerning the detection of surge and rotating stall in a compression system are considered. It is observed that, when surge or rotating stall happens, the plenum pressure rise and mass flow rate of a compression system exhibit abrupt change while those of its linearized model do not. With this observation, it is shown that the surge and rotating stall can be successfully detected by employing a linear-based fault identification filter (FIDF) design technique. This is achieved by treating the difference between the output of the compression system and that of its linearized model at an unstalled operating point as a fault vector and then investigating the effect of the fault on the designed FIDF. Simulation results with regard to Moore and Greitzer's compression model (1986) are given to demonstrate the effectiveness of the proposed approach. The theoretical study presented in this note may provide a guideline of detecting the occurrence of unstable phenomena at the onset so that corrective responses can be made in the practical applications.**

***Index Terms*—Fault identification filter, stall, surge.**

I. Introduction

In the recent years, it is known that the main obstacles to the high operating efficiency of a compression system are its instabilities. This has attracted considerable interest among engineers and researchers in the dynamic analysis and control design of such systems (see, e.g., [2]–[4], [9]–[14]). Compressed gas is subject to two main kinds of unstable behaviors: surge and rotating stall. The so-called "surge" is characterized as a one-dimensional mass wave motion while "rotating stall" is a wave-like disturbance propagating along the circumferential direction with constant rotating speed. Both of these two instabilities tend to raise the temperature in the compressor abruptly and may, in some cases, cause extreme mechanical damage. Therefore, distinguishing the causes of surge and rotating stall ([10]), detecting the inception of unstable phenomena (see, e.g., [4], [9], and [14]) and taking appropriate actions to prevent the instabilities (see, e.g., [2], [3], [10], and [12]) are all important issues.

Due to the growing demand for fault detection, diagnosis and identification of a control system, various techniques have been developed (see, e.g., [5]–[7] and the references therein). Among these techniques, the so-called "fault detection/identification filter" (FIDF) is one of the most effective (see e.g., [5] and [6]). Ding and Frank [6] proposed an algorithm for designing the FIDF by the use of factorization method in the frequency domain, while Chang *et al.* [5] employed the decoupling controller design concept to design the FIDF. The later design is easier to use since it does not require the computation of coprime factorization as mentioned in [6].

The main goal of this note is, from theoretical point of view, to show how the FIDF may be used to detect the occurrence of surge and rotating stall in a compression system. Strictly speaking, surge and rotating stall in a compression system are not faults in the usual sense (see, e.g., [6], [7]). However, when surge or rotating stall happens, it is observed that the plenum pressure rise and mass flow rate of the nonlinear compression system exhibit abrupt change while those of its linearized model do not. The idea behind this note is hence to treat the difference between the output of the compression system and that of its linearized model as a fault vector and inspect the influence of the fault vector on the residual of the FIDF. With the aid of a linear model-based FIDF design technique [5], the occurrence of surge and rotating stall is shown to be detectable by inspecting the residual generated from the FIDF. For practical applications, this study may provide engineers a signal for the time of taking appropriate control actions for preventing system instability. Since the employed FIDF technique is simple and easy to design, the proposed scheme in this note is then expected to be easier for physical implementation than the existing ones (see, e.g., [4], [9], [14]).

Manuscript received November 19, 1999; revised August 24, 2000. Recommended by Associate Editor M. Krstic. This work was supported by the National Science Council, Taiwan, R.O.C. under Grants NSC 88-2212-E-009-020, NSC 88-2212-E-009-022, NSC 89-2212-E-009-041, NSC 89-2212-E-009-042, and NSC 89-2212-E-009-044.

The authors are with the Department of Electrical and Control Engineering, National Chiao Tung University, Hsinchu 30039, Taiwan, R.O.C. (e-mail: dcliaw@cc.nctu.edu.tw).

Publisher Item Identifier S 0018-9286(01)09532-0.

II. The Fault Identification Filter (FIDF)

It is known that one of the most effective approaches to detect the appearance of faults in a control system is through the application of an FIDF (see, e.g., [5], [6]). In this section, the FIDF design presented in [5] is recalled, which will then be employed in Section III to detect the occurrence of surge and rotating stall in compression systems.

Consider a linear plant as given by

$$\dot{x}(t) = Ax(t) + Bu(t) + E_1 f(t) \tag{1}$$

$$\text{and } y(t) = Cx(t) + Du(t) + E_2 f(t) \tag{2}$$

where $x(t) \in \mathbf{R}^n$, $u(t) \in \mathbf{R}^m$, $f(t) \in \mathbf{R}^q$ and $y(t) \in \mathbf{R}^p$ denote the state vector, the input vector, the fault vector and the output vector, respectively. For simplicity and without loss of generality, we assume that $p = q$. The case for $p > q$ can be reduced to that of $p = q$ [5]. From (1) and (2), by taking Laplace transform, we have $y(s) = G_u(s)u(s) + G_f(s)f(s)$ with $G_u(s) = C(sI - A)^{-1}B + D$ and $G_f(s) = C(sI - A)^{-1}E_1 + E_2$. The objective of FIDF design is to construct two proper and stable filters $H_1(s)$ and $H_2(s)$ such that the residual vector

$$r(s) = H_1(s)u(s) + H_2(s)y(s) \tag{3}$$

has the following asymptotic property:

$$r(s) \longrightarrow 0 \text{ if and only if } f(s) \longrightarrow 0. \tag{4}$$

One of the existing results of FIDF design is recalled in Lemma 1 below.

Lemma 1 [5]: An FIDF with property (4) for the linear system (1) and (2) exists if A is a Hurwitz matrix and $G_f(s) = C(sI-A)^{-1}E_1 + E_2$ is invertible.

From the definition of $y(s)$, the residual vector in (3) can be rewritten as

$$r(s) = [H_1(s) + H_2(s)G_u(s)]u(s) + H_2(s)G_f(s)f(s). \tag{5}$$

The main idea behind the FIDF design is to delete the effects of the control input and nonzero initial state on the residual vector $r(s)$ while providing the fault signal $f(s)$ directly through the magnitude of $r(s)$. Based on the assumptions of Lemma 1, the FIDF design procedure given in [5] can then be summarized as the following algorithm.

Algorithm 1 (FIDF Design Procedure):

Step 1) Construct $H_2(s)$ so that the transfer matrix $H_2(s)G_f(s)$ is a diagonal proper and stable one.

Step 2) Determine $H_1(s)$ such that $H_1(s) + H_2(s)G_u(s) = 0$.

Step 3) Check the residual value from $r(s)$ by (3).

Note that, the system output affected by nonzero initial state will decay to zero since the system matrix A is required to be a Hurwitz ma-

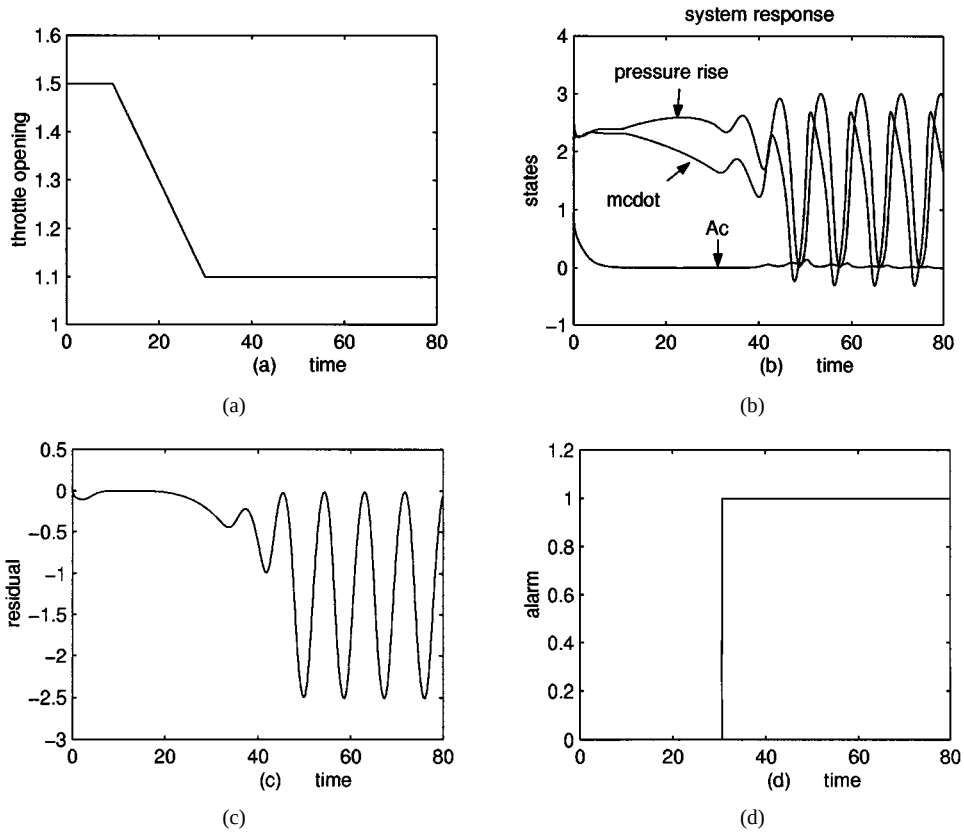

Fig. 1. (a) Control input. (b) Time response of system states. (c) Residual. (d) Alarm signal.

trix. Thus, the property (4) for system (1) and (2) can then be achieved via Algorithm 1.

It is known that the location of equilibrium points of a parameterized nonlinear system $\dot{x} = f(x, \mu)$ may vary as the parameter μ varies. The domain of attraction of the asymptotic stability equilibrium points then depend on the parameter μ and their locations. Although the domain of attraction of an asymptotically stable equilibrium point may be small so that small variation of the state can result in an undesired unstable behavior, while its linearized model at that equilibrium point is always globally asymptotically stable. This implies that the states of a nonlinear system and its linearization may exhibit dramatic different behavior due to the variation of system parameters and/or disturbance.

Now, we study the detection of the abrupt change of dynamical behavior for nonlinear system via FIDF design. Consider a nonlinear control model as given by

$$\dot{x} = h(x, u) \tag{6}$$

where $x \in \mathbf{R}^n$ and $u \in \mathbf{R}^m$ denote the state and control input, respectively. Note that, in general, the operating point of (6) depends on the value of control input u. In order to apply the FIDF results of [5], the linearized model of system (6) at an operating point (x^0, u^0) is constructed as

$$\dot{\hat{x}} = A\hat{x} + B\hat{u} \tag{7}$$

where $\hat{x} = x - x^0$, $\hat{u} = u - u^0$, $B = (\partial h/\partial u)(x^0, u^0)$ and $A = (\partial h/\partial x)(x^0, u^0)$ is assumed to be a Hurwitz matrix. Moreover, we assume that the available output for system (6) is in the form of

$$y = C\hat{x} + D\hat{u} \tag{8}$$

where $C \in \mathbf{R}^{p\times n}$ and $D \in \mathbf{R}^{p\times m}$ are two constant matrices.

Denote $y_{\rm non}(t)$ and $y_{\rm lin}(t)$, respectively, the output for nonlinear and linear model. It is noted that, in general, the two outputs $y_{\rm non}(t)$ and $y_{\rm lin}(t)$ are not equal. For the linearized model (7), it is known (e.g., [8]) that the steady-state output is linearly dependent on the input if A is a Hurwitz matrix. However, when the domain of attraction for the linearly stable operating point x^0 is not very large, the state of the nonlinear model might exhibit abrupt changed behavior. With these observations and taking the difference $y_{\rm non}(t) - y_{\rm lin}(t)$ as a fault vector $f(t)$, the FIDF technique is then employed to inspect the effect of this fault vector on the dynamics of system (1) and (2). By comparing system (7) and (8) with the form of (1) and (2), we then have $E_1 = 0$ and E_2 being the identity matrix. This implies that $G_f(s) = E_2$ for system (7) and (8). It is clear that assumptions of Lemma 1 hold. We then have the next result from Lemma 1.

Proposition 1: Consider system (6) and its linearized model (7) with the output being in the form of (8). Then an FIDF with property (4) exists for system (6) if A is a Hurwitz matrix.

III. Application to Compression Systems

In this section, the FIDF technique summarized in Proposition 1 will be employed to detect the occurrence of surge and rotating stall in a compression system. Strictly speaking, the surge and rotating stall phenomena in compression systems are not faults in the usual sense (see, e.g., [6], [7]). However, when surge or rotating stall happens, it is observed that the plenum pressure rise and mass flow rate of the compression system exhibit abrupt changed behavior while those of its linearized model do not. Given the significant difference between the states of the nonlinear and linearized models when surge or rotating stall occurs, it is shown below that the FIDF technique can be successfully employed to detect the occurrence of surge and rotating stall for compression systems. Details are given below.

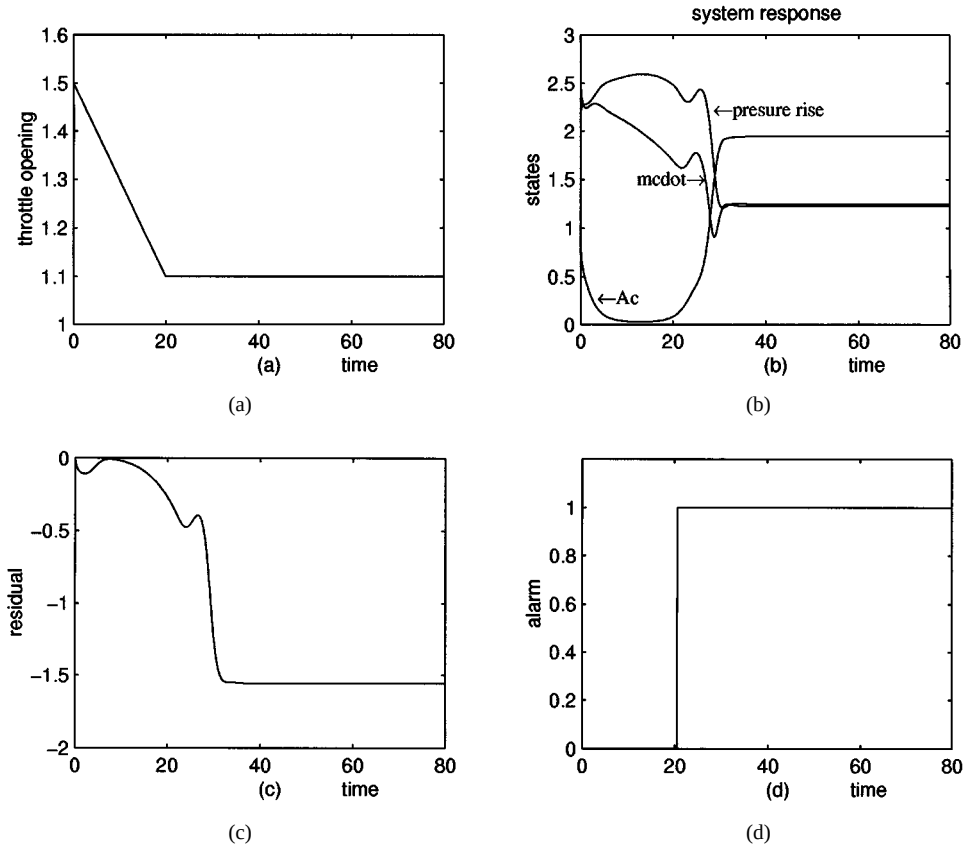

Fig. 2. (a) Control input. (b) Time response of system states. (c) Residual. (d) Alarm signal.

Consider a third-order compression system model introduced by Moore and Greitzer [13], given as follows:

$$\frac{dA_c}{dt} = \frac{\alpha}{\pi W}\int_0^{2\pi} C_{ss}(\dot{m}_c + WA_c\sin\theta)\sin\theta\, d\theta \tag{9}$$

$$\frac{d\dot{m}_c}{dt} = -\Delta P + \frac{1}{2\pi}\int_0^{2\pi} C_{ss}(\dot{m}_c + WA_c\sin\theta)\, d\theta \tag{10}$$

$$\frac{d\Delta P}{dt} = \frac{1}{4B_c^2}\left[\dot{m}_c - F(\gamma, \Delta P)\right]. \tag{11}$$

Here, we adopt the notations of [10]. In (9)–(11), A_c, $\dot{m}_c$ and ΔP denote the amplitude of the first harmonic of asymmetric flow, nondimensional compressor mass flow rate and nondimensional plenum pressure rise (or the so-called "total-to-static pressure-rise coefficient," see, e.g., [13]), respectively. Suppose the compressor characteristic C_{ss} is a smooth function. From (9), it is easy to check that $A_c = 0$ always results in $dA_c/dt = 0$. However, there may be equilibrium points of (9)–(11) for which $A_c \neq 0$ [10]. Denote $\left(0, \dot{m}_c^0(\gamma), \Delta P^0(\gamma)\right)^{\mathrm{T}}$ the so-called "unstalled equilibrium points." It is clear from (10) and (11) that $\dot{m}_c^0 = F(\gamma, \Delta P^0)$ and $\Delta P^0 = C_{ss}(\dot{m}_c^0)$. Note that, the location of the unstalled operating point of the system depends on the throttle control parameter γ.

Let $x = (x_1, x_2, x_3)^{\mathrm{T}}$ with $x_1 = A_c$, $x_2 = \dot{m}_c$ and $x_3 = \Delta P$. The linearized model of system (9)–(11) at an unstalled operating point $x^0(\gamma^0) = \left(0, \dot{m}_c^0(\gamma^0), \Delta P^0(\gamma^0)\right)^{\mathrm{T}}$ for some $\gamma = \gamma^0$ can be given in the form of (7) with $\hat{x} = x - x^0(\gamma^0)$, $\hat{u} = \hat{\gamma} = \gamma - \gamma^0$

$$A = \begin{pmatrix} \alpha C'_{ss}\left(\dot{m}_c^0(\gamma^0)\right) & 0 & 0 \\ 0 & C'_{ss}\left(\dot{m}_c^0(\gamma^0)\right) & -1 \\ 0 & \frac{1}{4B_c^2} & \Lambda \end{pmatrix} \tag{12}$$

$$B = \begin{pmatrix} 0 & 0 & -\frac{1}{4B_c^2}\frac{\partial F(\gamma^0, \Delta P^0(\gamma^0))}{\partial \gamma} \end{pmatrix}^{\mathrm{T}} \tag{13}$$

$$\text{and } \Lambda = -\frac{1}{4B_c^2}\frac{\partial}{\partial \Delta P}F\left(\gamma^0, \Delta P^0(\gamma^0)\right). \tag{14}$$

It was shown in [10] that the unstalled operating point $x^0(\gamma^0)$ is locally asymptotically stable (resp. unstable) for $C'_{ss}\left(\dot{m}_c^0(\gamma^0)\right) < 0$ (resp. $C'_{ss}\left(\dot{m}_c^0(\gamma^0)\right) > 0$). In addition, the rotating stall is found [12] to occur at $\gamma^0 > \gamma^s$ even with $C'_{ss}(\dot{m}_c^0(\gamma^0)) < 0$. Here, γ^s denotes the value of γ at which saddle node bifurcation occurs. As mentioned in [10] that $A_c = 0$ is an invariant manifold for system (9)–(11), the surge behavior can be observed from the reduced two-dimensional model as in (10) and (11) with $A_c = 0$ after the occurrence of Hopf bifurcation, see e.g., [1]. The Hopf bifurcation is known [10] to appear after the occurrence of stationary pitchfork bifurcation (i.e., the so-called "stall inception point"), at which $C'_{ss}\left(\dot{m}_c^0(\gamma^0)\right) = 0$. Based on the studies of the surge behavior in [1] and rotating stall in [10], an FIDF can then be constructed to detect the two instabilities of compression system (9)–(11). It is observed from (9)–(11) that the compressor model fits the form of (6), we then have the next lemma from Proposition 1.

Lemma 2: An FIDF with property (4) can be constructed for system (9)–(11) to detect the rotating stall (resp. surge behavior) if A in (12) is stable (resp. if the right bottom 2×2 submatrix of A is stable).

To demonstrate the application of the proposed methodology, in the following we present simulation results to verify the effectiveness of the approach. Let the axisymmetric compressor characteristic C_{ss} and the inverse of the throttle pressure rise map F be, respectively, adopted from [10] as $C_{ss}(\dot{m}_c) = 1.56 + 1.5(\dot{m}_c - 1) - 0.5(\dot{m}_c - 1)^3$ and $F(\gamma, \Delta P) = \gamma\sqrt{\Delta P}$. Moreover, the values of parameters α, W and B_c are from [10] as follows: $\alpha = 0.4114$, $W = 1$ and $B_c = 0.5$. It is known that the measurement of the state variable A_c is inherently noisy due to the intrusive nature of flow sensors (see, e.g., [2]).

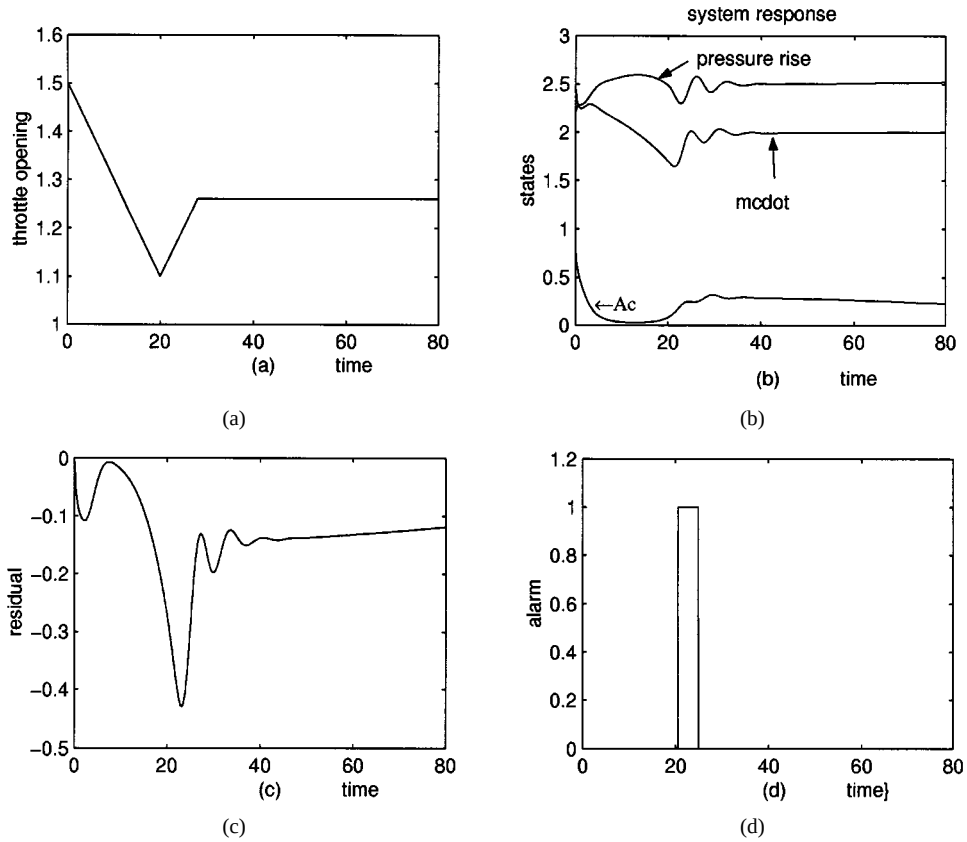

Fig. 3. (a) Control input. (b) Time response of system states. (c) Residual. (d) Alarm signal.

In this study, we assume that the available states for the compression system is ΔP only. The output is then chosen in the form of (8) with $C = (0\ 0\ 1)$ and $D = 0$ for both linear and nonlinear models of the compression system. It was shown from bifurcation analysis that the surge and rotating stall can occur only when $\gamma < \gamma^s = 1.463$ (see, e.g., [10], [12]). This motivates us to select the operating point at $\gamma^0 = 1.463$, which gives $x^0 = (0, 2.2809, 2.4306)^{\mathrm{T}}$. The matrix A given in (12) is found to be Hurwitz with eigenvalues $\{-0.3831; -0.6834 \pm 0.9688i\}$. Following the FIDF design procedure given in Algorithm 1, the two filters $H_1(s)$ and $H_2(s)$ in the FIDF are then designed for the linearized model (1) and (2) of system (9)–(11) as $H_1(s) = ((1.68s + 0.64)/((s + 1)(s^3 + 1.83s^2 + 2.02s + 0.57)), (1.60s^2 + 2.11s + 0.60)/((s + 1)(s^3 + 1.83s^2 + 2.02s + 0.57)))^{\mathrm{T}}$ and $H_2(s) = \mathrm{diag}\{1/(s + 1), 1/(s + 1)\}$. In the numerical simulations, the initial state is chosen as $(0.8, 2.5, 2.2)^{\mathrm{T}}$. The alarm signal is chosen to be 1 if $|\mathrm{residual}| > 0.3$ and equal to 0 elsewhere.

First, let the throttle opening be constant at 1.5 from $t = 0$ to $t = 10$ and decrease from 1.5 to 1.1 at $t = 30$ while maintaining that value thereafter as in Fig. 1(a). It is observed from Fig. 1(b) that both pressure rise ΔP and mass flow rate $\dot{m}_c$ oscillate after $t = 30$ while the amplitude of the first harmonic of asymmetric axis flow A_c almost retains at *zero* value. This implies that the system undergoes *surge* behavior, which starts after $t = 30$. The onset of surge becomes visible around $t \approx 30$ and is recognizable from the change in the residual and alarm as displayed in Fig. 1(c) and (d). Next, we let the throttle control γ be decreasing from the beginning of simulation and maintains at value 1.1 after $t = 20$ as in Fig. 2(a). It is observed from Fig. 2(b) that ΔP and $\dot{m}_c$ approach constant values while A_c grows rapidly after $t = 20$ and maintains a nonzero constant value after $t = 30$. This means that there is a traveling wave of gas around the annulus of the compressor, which is an unacceptable state of operation. Such symptom is reflected in the residual and alarm signal as in Fig. 2(c) and (d). Note that, the two simulations for detecting system instabilities agree with the results of Lemma 2. Finally, a control effort is attempted in Fig. 3(a) to recover from stall when an alarm signal is detected. From Fig. 3(b), the rotating stall behavior disappears and the state reaches an equilibrium point after a short time transient. This can also be seen from Fig. 3(c) and (d), where the alarm is turned off when the stall is recovered. Note that, due to the delay effect, although the alarm is turned off at about $t = 25$, the throttle should keep opening before $t = 28$ to avoid the growth of A_c. In fact, it is observed from numerical simulations that the slower the throttle is fixed at a constant value, the fast the state A_c converges to zero. Details are omitted. Nevertheless, this demonstrates that a proper control action can be applied to diminishing the surge or stall behavior when such instabilities are successfully detected. Another control strategy for stall recovery with the throttle opening being a function of the pressure rise can be found in [11].

IV. Conclusion

In this note, we have studied the detection of surge and rotating stall using a Moore and Greitzer's compression model. By treating the difference between the output of the compression system and that of its linearized model as a fault vector and employing a linear-based fault identification filter design technique, it is found that the surge and rotating stall can be successfully detected. By properly adjusting the threshold for generating the alarm signal, the FIDF may provide a precursor of avoiding undesirable system behaviors. Although the results in this note were obtained from theoretical study, they might provide a guideline in the real applications.

Acknowledgment

The authors are grateful to the reviewers for their helpful comments and suggestions.

REFERENCES

[1] E. H. Abed, P. K. Houpt, and W. M. Hosny, "Bifurcation analysis of surge and rotating stall in axial flow compressors," *ASME J. Turbomachinery*, vol. 115, pp. 817–824, 1993.

[2] O. O. Badmus, S. Chowdhury, K. M. Eveker, C. N. Nett, and C. J. Rivera, "Simplified approach for control of rotating stall part 1: Theoretic development," *J. Propulsion Power*, vol. 11, no. 6, pp. 1195–1209, 1995.

[3] O. O. Badmus, K. M. Eveker, and C. N. Nett, "Control-oriented high-frequency turbomachinery modeling: General one-dimensional model development," *ASME J. Turbomachinery*, vol. 117, pp. 320–335, 1995.

[4] M. M. Bright, H. K. Qammar, H. J. Weigl, and J. D. Paduano, "Stall precursor identification in high-speed compressor stages using chaotic time series analysis method," *ASME J. Turbomachinery*, vol. 119, no. 3, pp. 491–499, 1997.

[5] S.-K. Chang, P.-L. Hsu, and K.-L. Lin, "A parametric transfer matrix approach to fault-identification filter design and threshold selection," *Int. J. Syst. Sci.*, pp. 741–754, 1995.

[6] X. Ding and P. M. Frank, "Fault detection via factorization approach," *Syst. Control Lett.*, vol. 14, pp. 431–436, 1990.

[7] P. M. Frank and B. Köppen-Seliger, "Fuzzy logic and neural network applications to fault diagnosis," *Int. J. Approximate Reasoning*, vol. 16, pp. 67–88, 1997.

[8] B.-C. Kuo, *Automatic Control Systems*, 5th ed. Englewood Cliffs: Prentice Hall, 1987.

[9] P. B. Lawless, K. H. Kim, and S. Fleeter, "Characterization of abrupt rotating stall initiation in an axial-flow compressor," *J. Propulsion Power*, pp. 709–715, 1994.

[10] D.-C. Liaw and E. H. Abed, "Active control of compressor stall inception: A bifurcation-theoretic approach," *Automatica*, vol. 32, pp. 109–115, 1996.

[11] D.-C. Liaw and J.-T. Huang, "Fuzzy control for stall recovery in compressor dynamics," *J. Control Syst. Technol.*, vol. 6, no. 4, pp. 231–241, 1998.

[12] ——, "Global stabilization of axial compressors using nonlinear cancellation and backstepping design," *Int. J. Syst. Sci.*, pp. 1345–1361, 1998.

[13] F. K. Moore and E. M. Greitzer, "A theory of post-stall transient in axial compression systems. Part I—Development of equations," *ASME J. Engine Gas Turbines Power*, vol. 108, pp. 68–76, 1986.

[14] G. Vachtsevanos, H. Kang, J. Cheng, and I. Kim, "Detection and identification of axial flow compressor instabilities," *AIAA J. Guid., Control, Dyna.*, vol. 15, no. 5, pp. 1216–1223, 1992.

A New Controller Architecture for High Performance, Robust, and Fault-Tolerant Control

Kemin Zhou and Zhang Ren

***Abstract*—In this note, we propose a new feedback controller architecture. The distinguished feature of our new controller architecture is that it shows structurally how the controller design for performance and robustness may be done separately which has the potential to overcome the conflict between performance and robustness in the traditional feedback framework. The controller architecture includes two parts: one part for performance and the other part for robustness. The controller architecture works in such a way that the feedback control system will be solely controlled by the performance controller when there is no model uncertainties and external disturbances and the robustification controller will only be active when there are model uncertainties or external disturbances.**

***Index Terms*—Fault-tolerant control, H_∞ control, internal model control, robust control.**

I. INTRODUCTION

A fundamental reason for using feedback control is to achieve desired performance in the presence of external disturbances and model uncertainties. It is well known that there is an intrinsic conflict between performance and robustness in the standard feedback framework, see [3], [9], [11], [20], [21] for some detailed analyzes and discussions. In other words, one must make a tradeoff between achievable performance and robustness against external disturbances and model uncertainties. For example, a high-performance controller designed for a nominal model may have very little robustness against the model uncertainties and external disturbances. For this reason, worst-case robust control design techniques such as H_∞ control, L_1 control, μ synthesis, etc, have gained popularity in the last twenty years or so, see, for example, [1], [2], [6], [8], [13], [17], [20], [21] and references therein. Unfortunately, it is well recognized in the robust control community that a robust controller design is usually achieved at the expense of performance. This is not hard to understand since most robust control design techniques are based on the worst possible scenario which may never occur in a particular control system.

In this note, we shall propose a new controller architecture that has the potential to overcome the conflict between performance and robustness in the traditional feedback framework. This controller architecture uses the well-known Youla controller parameterization in a nontraditional way. The distinguished feature of our new controller architecture is that it shows structurally how the controller design for performance and robustness may be done separately. First of all, a high performance controller, say K_0, can be designed using any method, and then a robustification controller, say Q, can be designed to guarantee robust stability and robust performance using any standard robust control techniques. The feedback control system will be solely controlled by the high performance controller K_0 when there is no model uncertainties and external disturbances while the robustification controller

Manuscript received December 22, 1999; revised September 25, 2000 and February 1, 2001. Recommended by Associate Editor R. Tempo. This work was supported in part by ARO under Grant DAAH04-96-1-0193, the Air Force Office for Scientific Research under Grant F49620-99-1-0179, and LEQSF under Grant DOD/LEQSF(1996–99)-04.

K. Zhou is with the Department of Electrical and Computer Engineering, Louisiana State University, Baton Rouge, LA 70803 USA (email: kemin@ee.lsu.edu).

Z. Ren is with College of Marine Engineering, Northwestern Polytechnical University, Xian 710072, China (email: renzhag@nwpu.edu.cn).

Publisher Item Identifier S 0018-9286(01)09533-2.